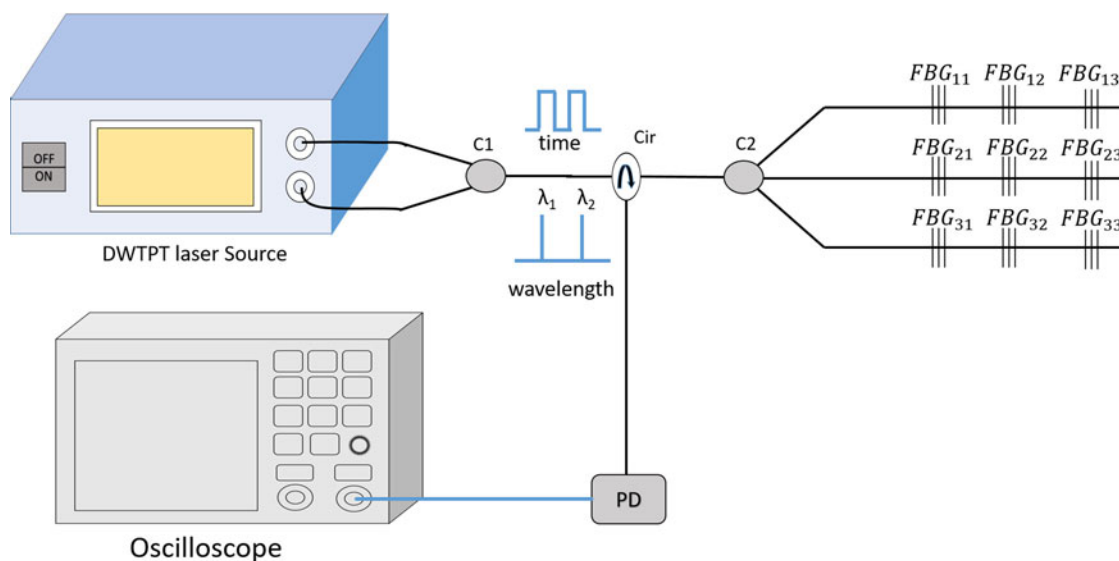


# TDM Interrogation of Identical Weak FBGs Network Based on Delayed Laser Pulses Differential Detection

Volume 10, Number 3, June 2018

Li Xia  
Ying Wu  
Udaya Rahubadde  
Wei Li



DOI: 10.1109/JPHOT.2018.2844779

1943-0655 © 2018 IEEE

# TDM Interrogation of Identical Weak FBGs Network Based on Delayed Laser Pulses Differential Detection

Li Xia , Ying Wu , Udaya Rahubadde , and Wei Li

School of Optical and Electronic Information, Huazhong University of Science and Technology, Wuhan 430074, China

DOI:10.1109/JPHOT.2018.2844779

1943-0655 © 2018 IEEE. Translations and content mining are permitted for academic research only.

Personal use is also permitted, but republication/redistribution requires IEEE permission.

See [http://www.ieee.org/publications\\_standards/publications/rights/index.html](http://www.ieee.org/publications_standards/publications/rights/index.html) for more information.

Manuscript received April 6, 2018; revised May 16, 2018; accepted June 4, 2018. Date of publication June 13, 2018; date of current version June 18, 2018. This work was supported in part by the National Natural Science Foundation of China under Grant 61675078; and in part by the subproject of the Major Program of the National Natural Science Foundation of China under Grant 61290315. Corresponding author: L. Xia (e-mail: xiali@hust.edu.cn).

**Abstract:** We report a time- and wavelength multiplexing sensing network based on nearly identical ultraweak fiber Bragg gratings (FBGs). In the multiplexing scheme of the network, each wavelength channel is distinguished by time delays of the two probe laser lines, and every channel works as an optical time domain reflectometry, and the response of each FBG is represented by two delay pulses corresponding to the two laser lines. The Bragg wavelengths of the FBGs are interrogated by calculating the ratio of two peak power of returned laser lines. Compared with a conventional wavelength scanning system, the proposed system can achieve relatively high interrogation speed. A proof of concept experiment with nine FBGs, at three wavelength channels was demonstrated, and fast measurements for static strain were achieved, with the sensitivity around  $-0.0023 \text{ dB}/\mu\epsilon$  and dynamic range over  $2500 \mu\epsilon$  for three channels.

**Index Terms:** Fiber Bragg gratings, demodulation, time-division multiplexing.

## 1. Introduction

Identical weak FBG based large scale sensing network has attracted great interests in quasi-distributed area, such as temperature, strain and structural health monitoring because of its low cost, low crosstalk and strong multiplexity [1], [2]. On-line grating writing system has been well developed in recent years, through which thousands of identical FBGs can be fabricated along a fiber [3]. Wavelength-division multiplexing (WDM) method and Time-division multiplexing (TDM) dominate application of the FBG sensing. A method using identical weak FBGs array called OTDR-FBG has been reported, in which different FBGs were distinguished by the reflected signal in time domain [4], [5]. They used a tunable laser diode (TLD) as light source to scan the whole spectrum of FBGs, and a highspeed data acquisition device was applied. By scanning the main lobe of FBGs with a 0.03 nm increment, the spectrum of all FBGs along the fiber were reconstructed. However, due to the slow wavelength scanning speed of TLD, there was a tradeoff between interrogation time and precision. Several kinds of semiconductor optical amplifier (SOA) resonant cavity based TDM sensing network was proposed [6]–[8]. The multiplexity capacity was limited by the ratio of SOA's gain and reflectivity of FBGs. The intensity-based interrogation method has attracted great

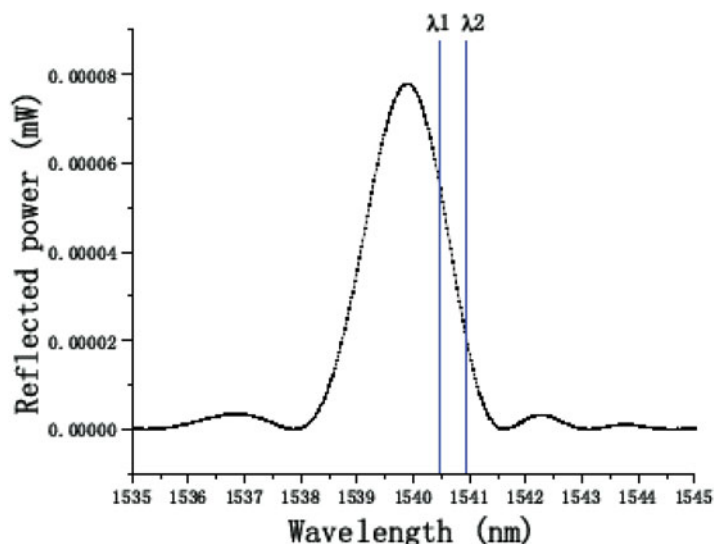


Fig. 1. FBG spectrum (black) and laser lines (blue).

interest, because of its simplicity in TDM sensing system. However, intensity-based interrogation suffers from source power fluctuation and optical loss along the transmission fiber [9].

A method based on shifted Gaussian filter was reported in [10]. By using differential detection technique, influence of power fluctuation can be well suppressed. However, low power spectrum density (PSD) of the ASE light source used in that method, restricts the multiplexing capability, sensing distance and dynamic range of the system. We demonstrate an intensity-based weak FBG interrogation system by using a dual-wavelength pulse laser source with programmable time delays, which fully eliminates the drawbacks mentioned above. The proposed method inherits the important features of differential detection technique, that is, natural insensitivity to power variations and propagation loss along the fiber. Different from tunable laser sweeping method, the proposed scheme just need two laser probe lines by taking full advantage of the Gaussian function of weak FBG spectrum, which can improve the interrogation speed significantly. By switching the laser lines to other wavelength channels, the sensor number can be further increased. Time delays can be set for different channels, thus we can distinguish channels by checking time domain signals. Furthermore, by injecting different laser lines with different time delay, slot efficiency was well improved, and interrogation speed will enhance greatly. In this work, two commercial low cost communication laser chips were directly driven by current to generate two probe pulses. The cost of the whole system is less than two thousand dollars, which is greatly deduced.

## 2. Sensing Concept

### 2.1 Dual-Wavelength Differential Detection Based Wavelength Interrogation

According to Fig. 1, the FBG reflected power of the laser source on photodetector is proportional to the overlap integral of the spectrum density function of the laser source and the reflection spectrum of the fiber Bragg grating [3]

$$I_r(\lambda_i) = \int_0^{\infty} R(\lambda) P(\lambda - \lambda_i) d\lambda \quad (1)$$

where  $P(\lambda - \lambda_i)$  and  $R(\lambda)$  are the laser power spectrum and the FBG reflection spectrum, respectively. Considering that the linewidth of the laser source is much narrower than the FBG spectrum linewidth, the laser spectrum 'P' is assumed to be a delta function, and for weak gratings, it was

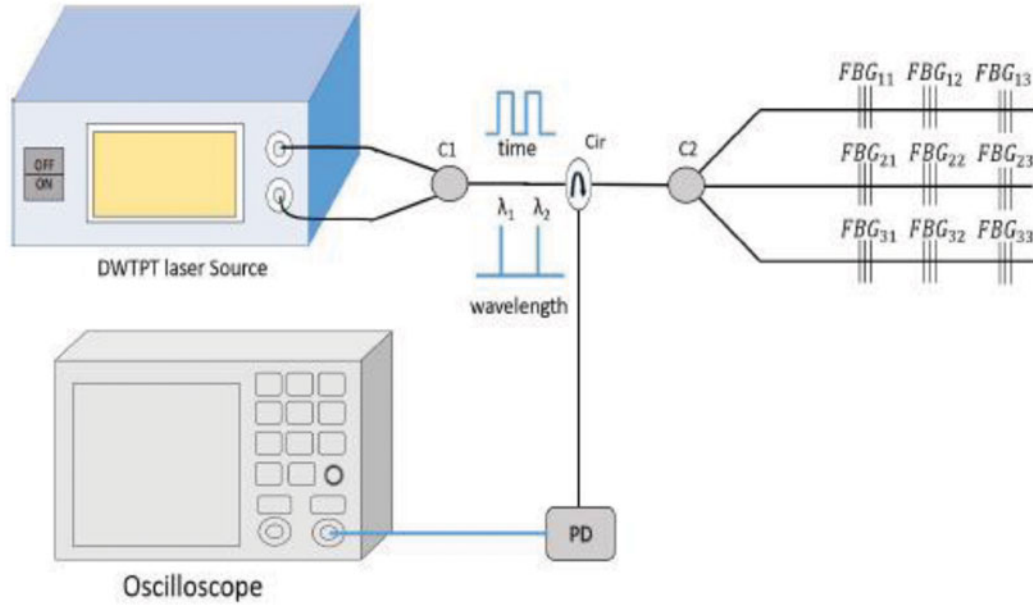


Fig. 2. Experimental setup of the differential demodulation strain sensing system. DWPTPT: Dual Wavelength Tunable Programmable Time delay laser source; PD: Photodetector; C1 and C2: 3 dB couplers; Cir: circulator.

suggested that the main lobe of the spectrum can be modeled as a Gaussian function [1], [2]:

$$R(\lambda) = R_o \exp\left(-4\ln 2 \left(\frac{\lambda - \lambda_B}{B_g}\right)^2\right) \quad (2)$$

where  $R_o$ ,  $\lambda_B$  and  $B_g$  are sensing FBG's peak reflectivity, Bragg wavelength and full width at half-maximum, respectively. Based on these two assumption, the reflected power can be expressed as:

$$I_r(\lambda_i) = C(\lambda_i) P(\lambda_i) R_o \exp\left(-4\ln 2 \left(\frac{\lambda_i - \lambda_B}{B_g}\right)^2\right) \quad (3)$$

where  $P(\lambda_i)$  is the laser power, and  $C(\lambda_i)$  describes the influences of the photoelectric conversion efficiency of the Photodetector and propagation loss. Thus, for a differential detection scheme, the power response of different laser line can be described as:

$$I_r(\lambda_1) = C(\lambda_1) P(\lambda_1) R_o \exp\left(-4\ln 2 \left(\frac{\lambda_1 - \lambda_B}{B_g}\right)^2\right) \quad (4)$$

$$I_r(\lambda_2) = C(\lambda_2) P(\lambda_2) R_o \exp\left(-4\ln 2 \left(\frac{\lambda_2 - \lambda_B}{B_g}\right)^2\right) \quad (5)$$

where  $\lambda_1$  and  $\lambda_2$  are the laser wavelength,  $C(\lambda_1) = C(\lambda_2)$ . So by subtracting the two Gaussian functions in the log-domain, that is,  $10 \log_{10} \left(\frac{I_r(\lambda_1)}{I_r(\lambda_2)}\right)$ , the measurement response of pulse power ratio (PPR( $\lambda_B$ )) can be obtained as:

$$\text{PPR}(\lambda_B) = E + F\lambda_B \quad (6)$$

where  $E = 10 \log_{10} \left(\frac{P(\lambda_1)}{P(\lambda_2)}\right) + (40 \log_{10} 2) \left(\frac{\lambda_2^2 - \lambda_1^2}{B_g^2}\right)$  and  $F = (-80 \log_{10} 2) \left(\frac{\lambda_2 - \lambda_1}{B_g^2}\right)$  are constant terms for each given case. As can be seen from Eq. (6), the differential result of weak FBG have an exactly

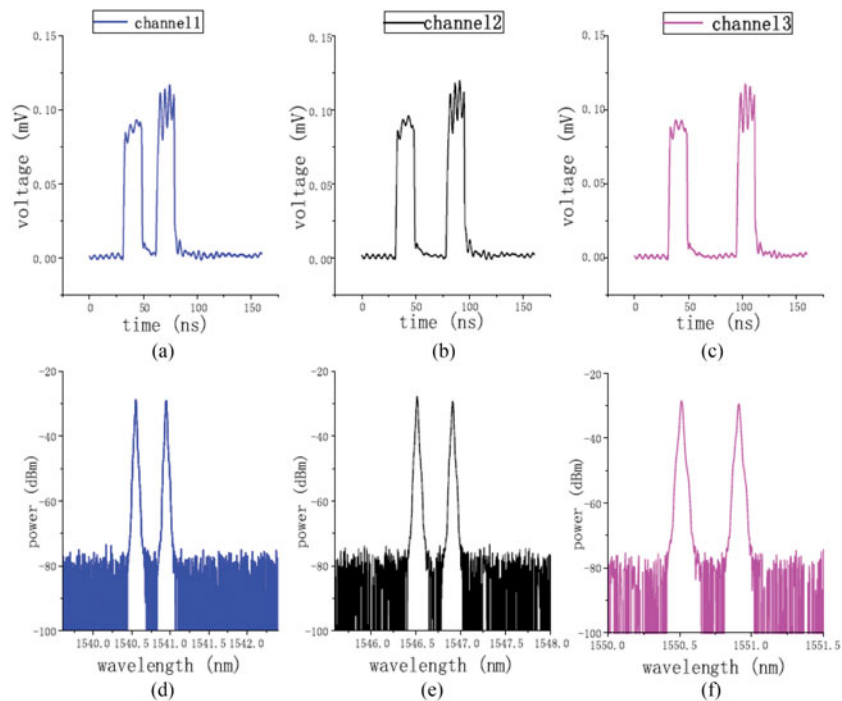


Fig. 3. Output characteristics of the DWTPT: (a) (b) (c) represent the time domain waveforms of three channels with different wavelength as (d) (e) (f) shows, respectively.

linear response with respect to the Bragg wavelength. In addition, benefiting from the differential detection, the readout is immune to propagation loss. The sensitivity is proportional to the wavelength space  $\lambda_1 - \lambda_2$ . Thus, the sensitivity can be easily changed by changing the spectrum spacing of two laser sources. From Fig. 1, we can see that the measuring range rely on the wavelength setting. For the strain sensing applications, the probe wavelengths should be located in the long wavelength region of the main lobe to obtain larger measuring range. For the vibration applications, the probe wavelengths should be located in the peak wavelength region of the grating spectrum to ensure enough dynamic range.

## 2.2 Sensing Network Interrogation

Our dual-wavelength Differential detection based FBG interrogation system scheme is illustrated in Fig. 2. The sensing network contains  $m$  sensing wavelength channels, and each channel has  $n$  identical weak FBGs. Light from a dual-wavelength pulse laser with programmable pulse width and delay time is launched into the sensing system. The reflected laser lines are received by the photodetector (PD) directly. A sampling oscilloscope is used to acquire the voltage signal from the PD.

## 3. Experiments

### 3.1 Experimental Setup

Our experimental system is depicted in Fig. 2. A dual-wavelength pulse laser source was used to generate two pulses with tunable pulse width, programmable delay time and tunable wavelength. The wavelength channels of the laser source were chosen based on the ITU grid. There are two directly modulated laser in the source. the wavelength and pulse can be changed quickly, and the wavelength tuning range can cover the whole C band while the delay time of the two pluses ranges from 0 to 1200 ns. As can be seen from Fig. 3. Three different delay time (40 ns, 60 ns, 80 ns)

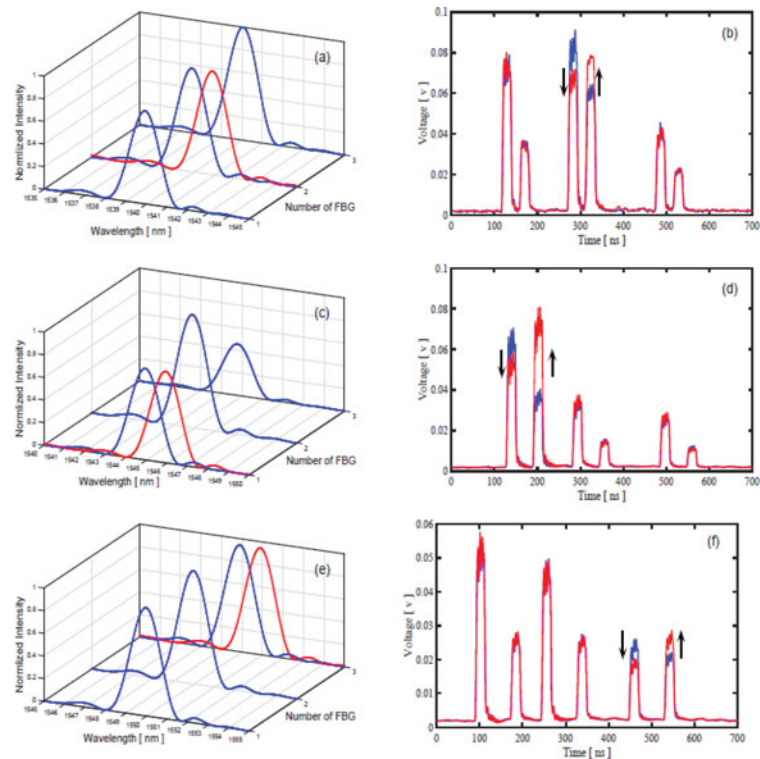


Fig. 4. Experimental result of demodulation system: a), c), e) represent the optical spectrum of channel 1540 nm, 1545 nm, 1550 nm, respectively. Strain were applied on FBG<sub>12</sub>, FBG<sub>21</sub>, FBG<sub>33</sub>. The blue curves and red curves represent experimental results in different strain. b), d), f) are experimental results in time domain corresponding to a), c), e), respectively.

correspond to three different wavelength channels (1540 nm, 1545 nm, 1550 nm) used in this experiment. A probe laser train with 20 ns pulse width and 10 kHz repetition rate was generated and injected into the sensing network. Three identical cascaded FBGs were used in each channel. The 3 dB bandwidth of FBGs we used were nearly 1.5 nm, and reflectivity were less than 7%. The fiber separation between two neighboring grating were 15 m. A 1 GHz APD (new focus 1647) were used for detection, and a sampling oscilloscope (Tektronix CSA7404) was used to acquire data.

As shown in Fig. 3(a)–(c), the voltage within one pulse range shows considerable fluctuations. This is because the pulses are directly modulated by the drive current, the impulse waveform is natively not a standard square wave because of the fluctuation of driving current and the rising edge jitter. During the practical measurements, the pulse voltage was averaged in the whole pulse duration time.

In the experimental setup, different identical FBGs in the same channel was distinguished by different time delays of the laser source, and two different laser line was separated by the initial time delays between them. This system was work as an OTDR for the scene of FBGs, and for the probe pulses with different wavelength, they were sampling in the wavelength domain but quantized in time domain. As shown in Eq. (6). The Bragg wavelength of each FBG was obtained by the differential output of two probe laser lines reflection. The laser wavelength for three channels were [1540.5 nm, 1540.9 nm], [1545.8 nm, 1546.2 nm], and [1550.5 nm, 1550.9 nm], respectively.

### 3.2 Experimental Results

Channel switching can be executed electronically but manually in our experiment, considering that oscilloscope was used for data acquisition. FBG<sub>12</sub>, FBG<sub>21</sub> and FBG<sub>33</sub> were glued to micrometric



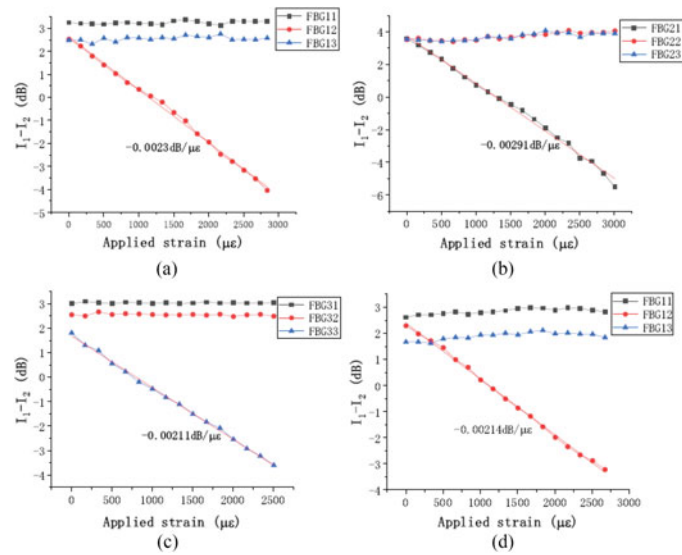


Fig. 5. Experimental results of the sensing system: a), b), c) represent channel 1540 nm, 1545 nm, 1550 nm, respectively. The power ratio ( $P_2/P_1$ ) of FBG<sub>12</sub>, FBG<sub>21</sub> and FBG<sub>33</sub> are decreasing linearly as the increasing strain applied, and d) shows the result of channel 1540 nm suffering from a propagation loss.

translation stage. Axial strains were applied to these FBGs. The stage has a resolution of 10  $\mu\text{m}$ . The reflection spectrum along each channel is shown by the left three inserts in Fig. 4. The red curves represent the spectrum under strains, which corresponds to the three right inserts that showed the reflected power changing. The sampling time was 800 ns, and the measurement of any sensing channel was averaged 250 times. Thus the sensing time was nearly 200  $\mu\text{s}$  for each channel. The relationship between the power substrate  $I_r(\lambda_1) - I_r(\lambda_2)$  and the strain is shown in Fig. 5. The blue, orange and gray plots represent the first, second, and third FBG in each channel, respectively. While strain was applied to FBG, the center wavelength will increase proportionally. In the meantime, the PPR( $\lambda_B$ ) decreases linearly according to Eq. (6). As can be seen from the linear curve fitting results, the sensitivity of FBG<sub>12</sub>, FBG<sub>21</sub>, FBG<sub>33</sub> was around  $-0.0023 \text{ dB}/\mu\epsilon$ ,  $-0.0023 \text{ dB}/\mu\epsilon$  and  $-0.0021 \text{ dB}/\mu\epsilon$ , and linear sensing range of 2800  $\mu\epsilon$ , 3000  $\mu\epsilon$  and 2500  $\mu\epsilon$  was obtained, respectively. As is shown in Eq. (6), the sensitivity and linear range can be changed easily by utilizing different laser lines, and there was a tradeoff between sensitivity and linear range. By bending the fiber before laser lines injecting to the system, and comparing the responses between insert (a) and insert (d), we proved that the sensing system was immunity to propagation loss along the fiber.

Moreover, the nonlinear curve with the strain applied FBG was caused by the inaccuracy of the applied strains and the environmental temperature drift. As for the fluctuate horizontal line with the non-strain applied FBGs, that is mainly caused by the crosstalk. While strains were applied to FBG<sub>21</sub>, the change of transmission loss for the two probe wavelengths are different. The power difference results for FBG<sub>22</sub> and FBG<sub>23</sub> show a rising trend. However, the power difference results for FBG<sub>31</sub> and FBG<sub>32</sub> are nearly constant while strain was applied to the last sensor FBG<sub>33</sub> in the channel.

### 3.3 Crosstalk

Assuming  $N$  identical weak FBGs was fabricated along a fiber, the reflected power from the  $i$ th ( $i = 1, 2, \dots, N$ ) FBG with laser line injection can be approximated from [11], [12]:

$$I_{ri} = (1 - R(\lambda_i))^{2i-2} R(\lambda_i) P(\lambda_i) \quad (7)$$

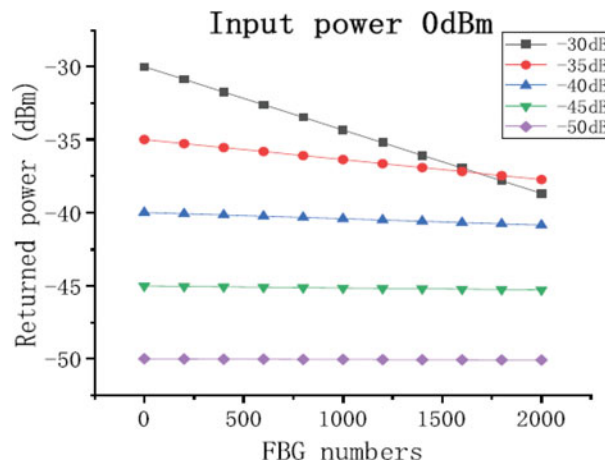


Fig. 6. Returning power of a 2000-FBG array with different reflectivity.

where  $P(\lambda_i)$  and  $R(\lambda_i)$  are the laser source power and spectrum reflectivity of the FBG, respectively. A returned power of each FBG in a 2000 FBG array was simulated, and the results of different reflectivity ranging from  $-30$  dB to  $-50$  dB was shown in Fig. 6. If the reflectivity is relatively high, the returned signal from the rear FBGs will be too low for detection. But when  $R_m$  is  $-50$  dB, the returned power from the 2000th FBG is nearly the same as the first one. In addition, the returned power from a special FBG in the array will be influenced by every FBG in front of it. For a large scale identical weak FBG sensing system, a correction is necessary for intensity based interrogation. In our experiment, for the  $i$ th FBG, the initial PPR, that is  $E$  in Eq. (6), decreases dramatically with  $i$  because of the FBG's reflectivity we used was 7%, relatively high. Another crosstalk named multiple reflections could induce an inevitable error in TDM sensing systems. But for an ultraweak identical FBG array, the crosstalk was negligible [12].

#### 4. Conclusion

We report a multi-wavelength channel weak FBG sensing network based on dual ports delayed pulses. Interrogation of each FBG was achieved by calculating the ratio of reflected power of two probe laser lines. By theoretical analysis, when the reflectivity is about  $-35$  dB, at least 2000 FBGs can be multiplexed in one channel, combined with WDM technique, that is switch wavelength channel in our system, the capability can be enhanced greatly. A proof of concept experiment with nine FBGs allocated to three wavelength channels has been demonstrated for fast static strain interrogation, with the sensitivity around  $-0.0023$  dB/ $\mu\epsilon$ , and dynamic range of over 2500  $\mu\epsilon$  for three channels, respectively.

#### References

- [1] S. J. Mihailov, "Fiber Bragg grating sensors for harsh environments," *Sensors*, vol. 12, no. 2, pp. 1898–1918, 2012.
- [2] G. Laffont, R. Cotillard, and P. Ferdinand, "Multiplexed regenerated fiber Bragg gratings for high-temperature measurement," *Meas. Sci. Technol.*, vol. 24, no. 9, 2013, Art. no. 094010.
- [3] H. Guo, F. Liu, Y. Yuan, H. Yu, and M. Yang, "Ultra-weak FBG and its refractive index distribution in the drawing optical fiber," *Opt. Exp.*, vol. 23, no. 4, pp. 4829–4838, 2015.
- [4] Y. M. Wang, J. M. Gong, D. Y. Wang, B. Dong, W. Bi, and A. Wang, "A quasi-distributed sensing network with time-division-multiplexed fiber Bragg gratings," *IEEE Photon. Technol. Lett.*, vol. 23, no. 2, pp. 70–72, Jan. 2011.
- [5] Y. M. Wang, J. M. Gong, D. Y. Wang, T. J. Shilig, and A. Wang, "A large serial time-division multiplexed fiber Bragg grating sensor network," *J. Lightw. Technol.*, vol. 30, no. 17, pp. 2751–2756, Sep. 2012.
- [6] Z. Luo, H. Wen, H. Guo, and M. Yang, "A time- and wavelength-division multiplexing sensor network with ultra-weak fiber Bragg gratings," *Opt. Exp.*, vol. 21, no. 19, pp. 22799–22807, 2013.



- [7] W. H. Chung and H. Y. Tam, "Time- and wavelength-division multiplexing of FBG sensors using a semi-conductor optical amplifier in ring cavity configuration," *IEEE Photon. Technol. Lett.*, vol. 17, no. 12, pp. 2709–2711, Dec. 2005.
- [8] Y. B. Dai, Y. J. Liu, J. S. Leng, G. Deng, and A. Asundi, "A novel time-division multiplexing fiber Bragg grating sensor interrogator for structural health monitoring," *Opt. Lasers Eng.*, vol. 47, no. 10, pp. 1028–1033, 2009.
- [9] P. Zhang, H. H. Cerecedo Nez, B. Qi, G. Pickrell, and A. Wang, "Optical time-domain reflectometry interrogation of multiplexing low reflectance Bragg-grating-based sensor system," *Opt. Eng.*, vol. 42, no. 6, pp. 1597–1603, 2003.
- [10] R. Cheng, L. Xia, Y. Ran, J. Rohollahnejad, J. Zhou, and Y. Wen, "Interrogation of ultrashort Bragg grating sensors using shifted optical Gaussian filters," *IEEE Photon. Technol. Lett.*, vol. 27, pp. 1833–1836, Sep. 2015.
- [11] D. J. F. Cooper, T. Coroy, and P. W. E. Smith, "Time-division multiplexing of large serial fiber-optic Bragg grating sensor arrays," *Appl. Opt.*, vol. 40, pp. 2643–2654, 2001.
- [12] Y. M. Wang, J. M. Gong, D. Y. Wang, B. Dong, W. Bi, and A. Wang, "A quasi-distributed sensing network with time-division-multiplexed fiber Bragg gratings," *IEEE Photon. Technol. Lett.*, vol. 23, no. 2, pp. 70–72, Jan. 2011.